ELSEVIER

Materials Science and Engineering A 460–461 (2007) 121–129

MATERIALS SCIENCE & ENGINEERING A

www.elsevier.com/locate/msea

Processing and microstructure of PCL/clay nanocomposites

Leandro N. Ludueña, Vera A. Alvarez, Analía Vazquez *

Research Institute of Material Science and Technology (INTEMA), National Research Council (CONICET), Engineering Faculty, National University of Mar del Plata, Av. J.B. Justo 4302, 7600 Mar del Plata, Argentina

Received 21 July 2006; received in revised form 4 January 2007; accepted 28 January 2007

Abstract

The morphology and mechanical properties of polycaprolactone/clay nanocomposite films prepared by two techniques (casting: exfoliation-adsorption; intensive mixing: melt-intercalation) were studied. Casting, which is a laboratory scale technique, was selected because it was supposed that the exfoliation of the layered silicate into single layers would be easier since the solvent acts as an exfoliation agent. The other selected technique was chosen because it can be used in the industry. X-ray diffractograms revealed an intercalated–exfoliated mixed structure for both techniques. For casting, the morphology and mechanical properties are influenced by the used solvent and the preparation conditions being the first one the most critical parameter. Otherwise, in the case of intensive mixing, a higher clay dispersion degree was produced by shear forces and the resultant mechanical properties were superior to those obtained by casting. In both cases, the highest modulus was achieved for 5 wt.% of C30B. Finally, an effective filler-parameters model was used to compare the relative dispersion of clay within the nanocomposites for both processes from the experimental modulus values.

Keywords: Nanocomposites; Biodegradable; Polycaprolactone; Clay; Silicate; Montmorillonite

1. Introduction

Packaging is the biggest industry of polymer processing. Food industry is its principal customer. Despite environmental problems, polymer packaging European market is increasing in about millions of tons per year. Foreseeing future laws about reducing the weight and volume of packaging products, cheap and biodegradable polymeric products are receiving growing attention [1]. Polycaprolactone (PCL) belongs to this class of synthetic biodegradable polymers. PCL is a linear, hydrophobic and partially crystalline polyester that can be slowly consumed by micro-organisms [2]. Its physical properties and commercial availability makes it a good substitute for conventional non-biodegradable polymers used not only for common applications but also for specific areas such as medicine and agriculture [3]. The performance of PCL can be greatly enhanced by the dispersion of nanometer-size particles [4]. The aim of reinforcing polymer materials has been to increase properties such as heat, mechanical and impact strength or to diminish some else such as electric conductivity and gases permeability. These reinforced materials mostly lack from an intense interaction at the interface of both components. In general, macroscopic reinforcing elements contain defects, which are less important as the element size becomes smaller. Nanocomposites are particle-filled polymers for which at least one dimension of the dispersed particles is in the nanometer range. The layered silicates commonly used in nanocomposites consist of two-dimensional layers, which are 1 nm thick and several microns long depending on the particular silicate. Three main types of composite may be obtained from the interaction between layered silicates and polymer chains: intercalated nanocomposites, exfoliated nanocomposites, microcomposites. Intercalated structures show regularly alternating layered silicates and polymer chains in contrast to exfoliated structures in which the individual clay layers are delaminated and dispersed in the polymer matrix. These two situations can however, coexist in the same material. When the polymer is unable to intercalate between the silicate sheets a traditional microcomposite is obtained [5].

Nanocomposites are almost obtained by the intercalation of the polymer (or a monomer subsequently polymerized) inside the galleries of layered crystals. Layered silicate nanocomposites have been more widely investigated probably because the starting clay materials are easily available and because their intercalation chemistry has been studied for a long time. Owing

* Corresponding author. Tel.: +54 223 481 6600; fax: +54 223 481 0046.
E-mail address: anvazque@fi.mdp.edu.ar (A. Vazquez).

0921-5093/$ – see front matter © 2007 Elsevier B.V. All rights reserved.
doi:10.1016/j.msea.2007.01.104

to the nanometer-size particles obtained by dispersion, this nanocomposites exhibit markedly improved mechanical, thermal and vapor barrier properties [5]. The exfoliation of layered minerals and hence the preparation of a homogeneous nanocomposite material is seriously rendered by the fact that sheet-like materials display a strong tendency to agglomerate as a consequence of their big contact surfaces and, so that, instead of totally exfoliated structures, intercalated nanocomposites (when the silicate layers are intercalated between polymer chains) are generally achieved [6].

Montmorillonite, hectorite and saponite are the most commonly used layered silicates due to their small particle size and their intercalation properties. Moreover economic and environmental factors, their natural abundance and their high mechanical and chemical strength make these layered silicates useful as reinforcing particles of polymer materials.

Although several strategies have been considered to prepare polymer/layered silicate nanocomposites, there are two main used techniques in the literature: casting and intensive mixing.

Casting produces exfoliation of the layered silicate into single layers by using a solvent in which the polymer is soluble. Layered silicates can be easily dispersed by the presence of the solvent, owing the weak forces that stack the layers together. The polymer then adsorbs onto the delaminated sheets and when the solvent is evaporated, the sheets reassemble, sandwiching the polymer to form an ordered multilayer structure. This technique has been widely used with water-soluble polymers to produce intercalated nanocomposites [7]. PEO has been successfully intercalated in sodium montmorillonite and sodium hectorite by dispersion in acetonitrile [8], allowing incorporating one or two polymer chains in between the silicate layers and increasing the interlayer spacing of the clays used. Jimenez et al. [9] have applied the casting method for the production of poly(ε-caprolactone) biodegradable nanocomposite using montmorillonite modified with distearyldimethylammonium cations. The composites were prepared by dissolving poly(ε-caprolactone) in hot chloroform in presence of a given amount of the modified clay, then vaporizing the solvent to obtain homogeneous films. However, under those conditions, it was found that no intercalation takes place in the presence of the polyester.

Intensive mixing is based on mixing the layered silicate with the polymer matrix in the molten state. Under these conditions and, if the layer surfaces have enough compatibility with the chosen polymer, the polymer can crawl into the interlayer spacing and form either an intercalated or exfoliated nanocomposite. Vapor barrier properties of poly(ε-caprolactone)/clay nanocomposites prepared by intensive mixing, have been improved in comparison to the neat polymer due to an exfoliated clay structure [10]. Lepoittevin et al. [1] obtained poly(ε-caprolactone)/clay nanocomposites by intensive mixing using organo-modified montmorillonite and sodium montmorillonite. In this case, only the organo-modified clay was able to produce an intercalated/exfoliated structure, while the natural sodium clay formed a conventional composite with micron-sized particles dispersed in the neat polymer. Homminga et al. [11] have studied the role of shear forces on the transformation of the original large clay agglomerates into polycaprolactone and other polymers. They found that shear forces in the melt-preparation of polymer layered mineral nanocomposites facilitate the break-up of large-sized agglomerates, but further exfoliation of the mineral layers is determined by the compatibility between the polymer matrix and the mineral layers rather than by shear forces.

The aim of this work was to study the relationship between morphology and mechanical properties of biodegradable polymer/clay nanocomposites prepared by two common used techniques: Casting (laboratory scale) and intensive mixing (for industrial applications). There are no works in the literature that compares similar materials obtained by different techniques and we consider that this study is really important due to the dissimilar morphologies developed in each case that also derived in materials with unlike properties, and, so that, appropriate or not for several applications.

2. Experimental

2.1. Materials

Polycaprolactone (PCL) Mn = 80,000, supplied by Aldrich, was used as a matrix. A commercial modified montmorillonite "Cloisite 30B" (C30B), supplied by Southern Clay Products Inc., was used as nanofiller. It is a natural montmorillonite modified with a methyl, tallow, bis-2-hydroxyethyl, quaternary ammonium. The modifier concentration was 90 mequiv./100 g clay. Clay moisture content was <2 wt.% and its specific gravity was 1.98 g/cm^3. Interlayer spacing d_{001} was 1.85 nm.

2.2. Sample preparation

Fig. 1 shows the schemes of procedures used to obtain nanocomposite films by each method.

In the case of casting (Fig. 1a), films of 0.11 mm thick with a clay content of 5 wt.% were obtained by using two solvents (dichloromethane and a 50% (v/v) dichloromethane–dimethylformamide mixture) and several ultrasonic bath times (5, 10, 15 and 20 min) in order to obtain the best mechanical performance.

Once obtained the best solvent and the optimal ultrasonic bath time, films with 0, 3.75, 5.0, 7.5 and 10.0 wt.% of clay, named PCL, 3.75C30B, 5C30B, 7.5C30B and 10C30B, respectively, were prepared at these conditions. The first numbers of the abbreviations correspond to the weight percent of clay and the last three characters correspond to the Cloisite name.

Nanocomposites with a clay content of 0, 2.5, 5.0 and 7.5 wt.% (PCL, 2.5C30B, 5C30B, 7.5C30B) were prepared by intensive mixing, and films 0.4 mm thick were performed by compression molding (Fig. 1b).

2.3. Free swelling

Two grams of C30B were slowly introduced into a graduated test tube containing 100 ml of organic solvent. Solvents used were dichloromethane, dimethylformamide and a 50%

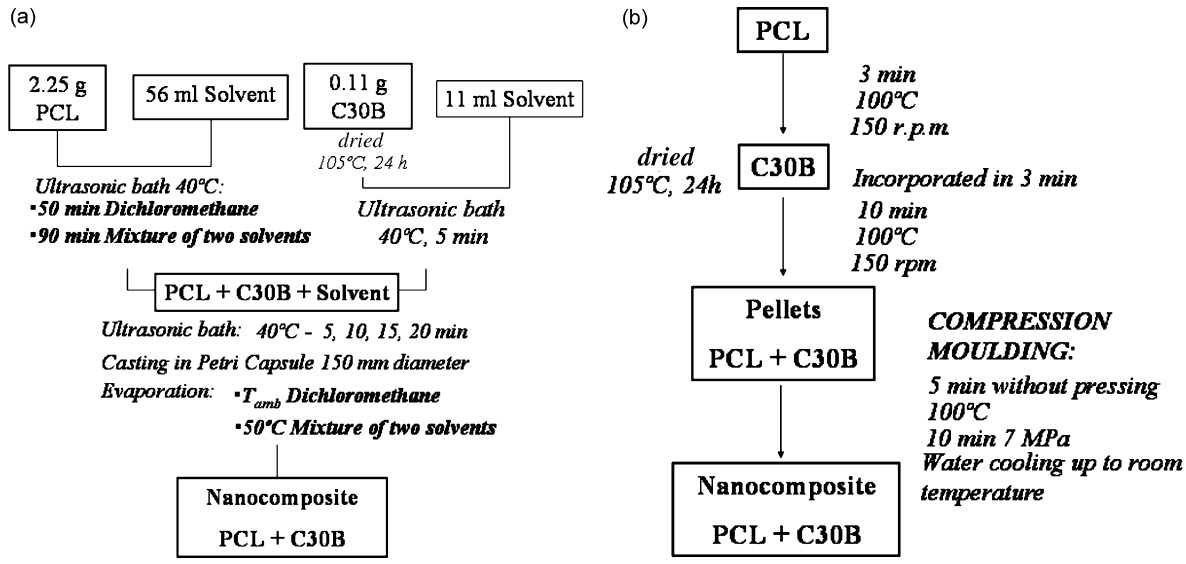

Fig. 1. Procedures to prepare nanocomposite films: (a) casting and (b) intensive mixing.

(v/v) solution of them. After 24 h, the volume of the suspension formed at room temperature, without any mixing, was measured.

2.4. Mechanical properties

Tensile tests were performed in a universal testing machine Instron 4467 at a constant crosshead speed of 50 mm/min. Samples were prepared according to the ASTM D882-91 standard. Before tests, all specimens were preconditioned at 65% RH (relative humidity). Tests were carried out at room temperature.

2.5. Differential scanning calorimetry (DSC)

Tests were performed in a Shimadzu DSC-50 from 25 to 100 °C at a heating rate of 10 °C/min under nitrogen (ASTM D3417-83). The degree of crystallinity was calculated from the following equation [12]:

$$X_{cr}\,(\%) = \frac{\Delta H_f}{w_{PCL}\,\Delta H_{100}} \times 100 \quad (1)$$

where ΔH_f is the experimental heat of fusion, w_{PCL} the PCL weight fraction and ΔH_{100} is the heat of fusion of 100% crystalline PCL and its value is 136.1 J/g [12].

2.6. Thermogravimetry analysis (TGA)

TGA measurements were carried out by using a Shimadzu TGA-50. The samples were heated from 25 to 1000 °C at a heating rate of 10 °C/min under nitrogen. The clay content was measured from the residual left at 410 °C.

2.7. Microscopy

Scanning electron microscopy (SEM) observations were performed with a JEOL JSM-6460 LV. The samples were fractured in liquid air, in order to avoid the surface deformation, and then gold-coated.

The surface of the films was observed by optical microscopy with an Olympus SZH 10.

2.8. X-ray diffractometry

Clay dispersion was analyzed by X-ray diffractometry. X-ray diffractograms were recorded by a PW1710 diffractometer equipped with an X-ray generator ($\lambda = 0.154060$ nm). Samples were scanned in 2θ ranges from 2° to 60° by a step of 0.035°.

3. Results and discussion

3.1. PCL/clay nanocomposite films obtained by casting

3.1.1. PCL dissolution

Three different solvents were used to dissolve PCL: chloroform, dichloromethane and dioxane. Solutions of each solvent with a PCL content of 0.3% (w/v) were put in ultrasonic bath for 50 min at 40 °C. Only dichloromethane was able to totally dissolve the polymer in the proposed conditions. Once obtained the best solvent, the minimal content for total dissolution was searched, resulting in 4% (w/v) solutions.

3.1.2. Free swelling characterization

The aim of preparing nanocomposites by casting is that the solvent used to dissolve the polymer, be also able to increase the interlayer spacing for subsequent intercalation of the polymer. For this purpose, free swelling of C30B was studied in dichloromethane, dimethylformamide and a 50% (v/v) solution of them. Dimethylformamide did not dissolve PCL in the proposed conditions, but Burgentzlé et al. [13] founded that it produces a great macroscopic and microscopic swelling of C30B, so it was used as a reference for the other solvents. After 24 h of free swelling, two phases can be observed in the test tubes. The first phase consists on a clay–solvent suspension and the other one is pure solvent. In order to compare the different

Table 1
Free swelling factor, S, of C30B in different solvents

Solvent	S
Dichloromethane	22
Dimethylformamide	97
50% (v/v) solution of the two solvents	89

Table 3
Average size and number of holes for matrix and 5C30B nanocomposites prepared by casting with dichloromethane

Material	Average size (mm)	Number of holes (n/mm^2)
PCL	0.27	0.07
5C30B	0.17	3.4

swollen volumes, V_s, defined as the volume of the slurry, it is necessary to take into account the volume of the dry powder, V_c. The free swelling factor, S, can be defined by the following equation [13]:

$$S = \frac{V_s - V_c}{V_c} \quad (2)$$

One can note that for S equal to 0, the nanoclays are not swollen by the solvents whereas for S equal to 1, the volume is twice the initial volume of the nanoclay powder. S values represent swelling at the macroscopic scale but an increasing interlayer spacing is not always related to it. Nevertheless, one can expect that if the free swelling factor values are high, the clay/solvent interaction is good. Free swelling factors, S, for the three solvents are shown in Table 1. The highest value of S was reported for dimethylformamide as was expected from Burgentzlé et al. results [13]. Free swelling factor, S, for the 50% (v/v) solution of dichloromethane and dimethylformamide was near to that for dimethylformamide, so two results are expected using the mixture of solvents: (1) easy dissolution of PCL and (2) good clay/solvent interaction.

3.1.3. Mechanical properties

Table 2 shows the mechanical properties for the matrix and 5C30B nanocomposites prepared with dichloromethane and the solution of two solvents at different ultrasonic bath times. Young's modulus was the only mechanical property improved by clay incorporation in comparison to the matrix, so the optimal ultrasonic bath time was chosen as the time for the highest modulus for which the decrease in the other two properties (strength and elongation at break) was acceptable. Thus, the highest Young's modulus of 5C30B nanocomposites was obtained with the mixture of solvents for 15 min of ultrasonic bath as reported in Table 2.

Fig. 2 show the optical micrographies of the evaporation surface for the matrix (Fig. 2a) and for 5C30B nanocomposites with 10 min of ultrasonic bath (Fig. 2b), both prepared with dichloromethane. These pictures reveal the tendency of the solvent to leave holes into the matrix during its evaporation. Pictures for 5C30B nanocomposites prepared with dichloromethane at 5, 15 and 20 min of ultrasonic bath were similar than Fig. 2b. Table 3 shows the average number and size of holes from different zones of four pictures of these nanocomposites. As all data lied within the same range of values, the average of all ultrasonic bath times was studied. The presence of clay increased the number of holes, while its size remained unchanged. The clay particles dispersed in the polymer solution could be acting as nucleation points for bubbles producing an increment in the number of defects and hence, a lower Young's modulus with respect to the matrix. Neat PCL and 5C30B nanocomposites prepared with the solution of two solvents did not display these holes as observed in optical microscopy pictures and confirmed with SEM micrographs (Fig. 3).

Differences in the surface morphology can be attributed to the boiling temperature (T_b) of the solvents (40 °C for dichloromethane and 153 °C for dimethylformamide). The lower the T_b, the faster the evaporation rate. It was confirmed with the time required to extract the films from the Petri capsules after casting (6 h at room temperature for dichloromethane, 24 h at 50 °C for the mixture of two solvents). When the mixture of solvents was used, the first one to evaporate was dichloromethane. Once all dichloromethane was evaporated, dimethylformamide, PCL and clay remained in the Petri capsules. It was observed that in the presence of dimethylformamide the polymer adopts a rubbery like state, without crystallizing. That state allows bubbles to achieve the surface and disappear while dimethylformamide is still evaporating. Dimethylformamide does not produce holes after its evaporation since its T_b is higher in comparison to dichloromethane. When only dichloromethane was used, PCL crystallizes immediately after its evaporation and hence, holes do not have enough time to achieve the surface and disappear due to the faster evaporation rate, so they remain as defects in the surface.

With the optimal conditions (mixture of two solvents, 15 min of ultrasonic bath), the influence of clay content on mechanical properties was evaluated. The highest Young's modulus and

Table 2
Mechanical properties for matrix and 5C30B nanocomposites prepared by casting with dichloromethane (SV1) and 50% (v/v) solution of solvents (SV3)

Material	$t_{ultrasonic\ bath}$ (min)	Young's modulus (MPa)		Strength (MPa)		Elongation at break (%)		ΔH_f (J/g)		X_{cr} (%)	
		SV1	SV3	SV1	SV3	SV1	SV3	SV1	SV3	SV1	SV3
PCL	0	434 ± 28	405 ± 18	28.5 ± 7.5	40.0 ± 8.0	540 ± 142	668 ± 90	89.6	81.9	63	58
5C30B	5	364 ± 15	537 ± 51	12.0 ± 1.5	22.0 ± 8.0	156 ± 140	440 ± 135	80.7	71.4	60	53
5C30B	10	372 ± 60	520 ± 11	10.0 ± 0.5	25.0 ± 1.0	72 ± 18	507 ± 48	75.7	79.5	56	59
5C30B	15	407 ± 26	596 ± 47	18.0 ± 2.5	24.0 ± 2.0	389 ± 51	445 ± 26	84.9	80.2	63	59
5C30B	20	367 ± 44	563 ± 21	13.0 ± 2.0	29.5 ± 6.5	234 ± 105	545 ± 105	74.6	83.2	55	62

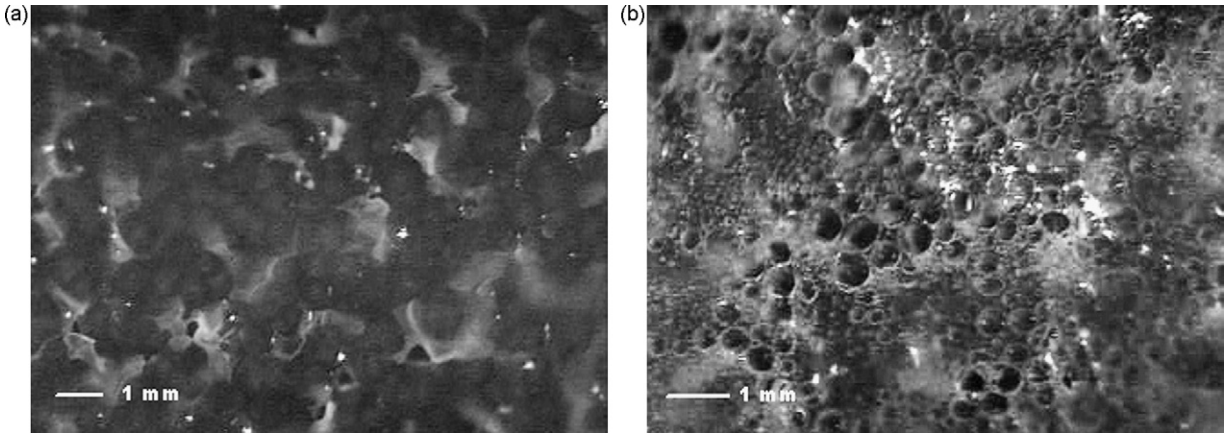

Fig. 2. Optical microcopy pictures showing the evaporation surface morphology of films prepared by casting with dichloromethane: (a) PCL and (b) 5C30B nanocomposite at 10 min of ultrasonic bath.

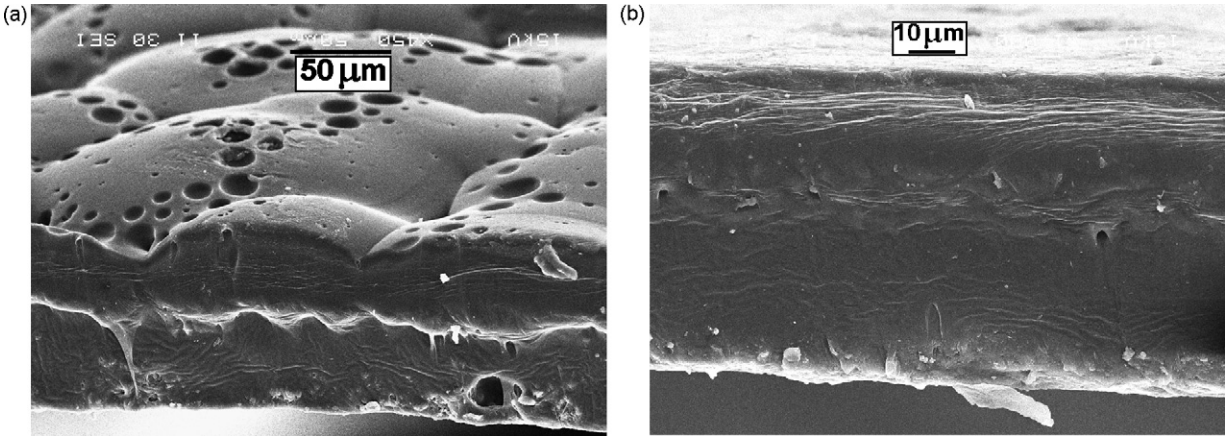

Fig. 3. SEM micrographs showing the evaporation surface morphology of 5C30B films prepared by casting: (a) dichloromethane, 15 min ultrasonic bath; (b) 50% (v/v) solution of solvents, 10 min ultrasonic bath.

the lower diminution on tensile strength and elongation at break were achieved with 5C30B nanocomposites (Table 4). Optical microscopy pictures showed the absence of defects in the evaporation surface for all weight percent of clay studied in the optimal conditions by casting.

3.1.4. Crystallinity

Crystallinity could be affecting mechanical properties since a higher fraction of crystals produces an increment in the strength and modulus of the material [14].

Table 2 shows the degree of crystallinity for the matrix and for the 5C30B nanocomposites prepared with dichloromethane and the mixture of solvents at different ultrasonic bath times. Table 4 lists the same property for nanocomposites prepared in the optimal conditions with different clay contents. It can be seen that the degree of crystallinity remained almost unchanged in the presence of clay for all ultrasonic bath times and clay contents studied.

3.1.5. Nanocomposites structure

The critical parameter to achieve the best performance of polymer/clay composites, if clay does not produce defects, is the clay dispersion. X-ray diffractometry was used in order to identify intercalated structures. In such nanocomposites, the

Table 4
Mechanical properties and degree of crystallinity from DSC analysis for matrix and their clay nanocomposites prepared by casting in the optimal conditions (50% (v/v) solution of solvents; 15 min ultrasonic bath)

Material	Young's modulus (MPa)	Strength (MPa)	Elongation at break (%)	ΔH_f (J/g)	X_{cr} (%)
PCL	405 ± 18	40 ± 8	668 ± 90	81.85	58
3.75C30B	390 ± 51	12 ± 1	230 ± 50	77.06	56
5C30B	596 ± 47	24 ± 2	445 ± 26	84.86	63
7.5C30B	484 ± 21	19 ± 2	441 ± 118	79.28	60
10C30B	468 ± 56	12 ± 1	225 ± 12	79.67	62

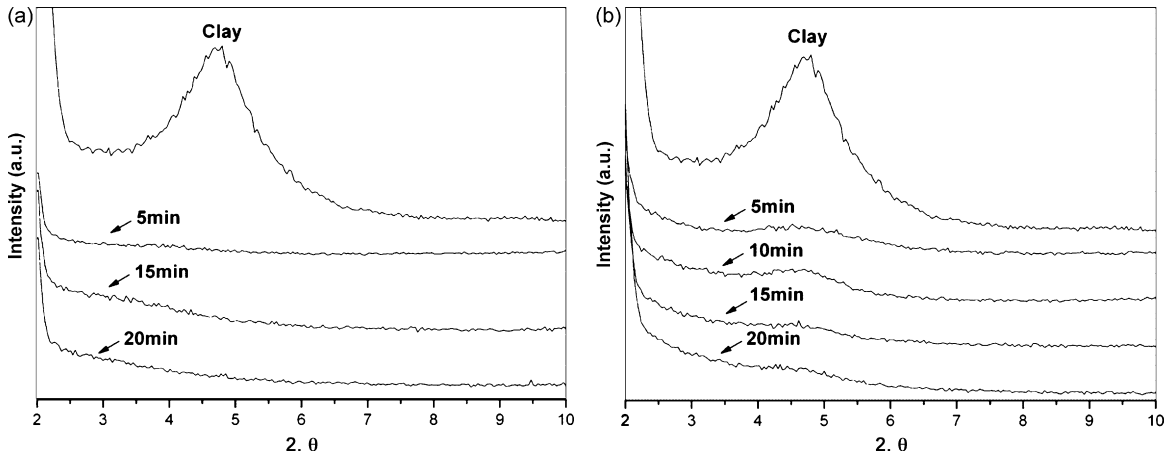

Fig. 4. X-ray diffractograms for 5C30B nanocomposites prepared by casting at different ultrasonic bath times: (a) dichloromethane and (b) mixing of solvents.

repetitive multilayer structure is well preserved, allowing the interlayer spacing to be determined. The intercalation of the polymer chains usually increases the interlayer spacing, leading to a shift in the diffraction peak towards lower angle values. As far as dispersion of clay becomes higher, no more diffraction peaks are visible in the X-ray diffractograms either because of a too much large spacing between the layers or because nanocomposites do not present ordering anymore. Besides these two well-defined structures, other intermediate organizations can exist showing both intercalation and exfoliation. In this case, a broadening of the diffraction peak is often observed [5]. Fig. 4 shows that both clay structures, intercalated and exfoliated, coexisted in 5C30B nanocomposites prepared with dichloromethane (Fig. 4a) and the mixture (50% v/v) of the two solvents (Fig. 4b) at all ultrasonic bath times, since a broadening on the diffraction peak in comparison with the clay alone was observed. The same results were obtained for 3.75C30B, 7.5C30B and 10C30B nanocomposites prepared by casting in the optimal conditions (mixture of solvents, 15 min of ultrasonic bath).

Fig. 5 shows SEM micrographs of the 5C30B nanocomposites thickness prepared with dichloromethane (Fig. 5a) and the mixture of solvents (Fig. 5b) with 15 min of ultrasonic bath. SEM micrographs for dichloromethane and the solution of solvents at 5, 10 and 20 min of ultrasonic bath were similar than Fig. 5a and b, respectively. In the case of dichloromethane, clay particles with a size range of 800–2100 nm were observed while for the mixing of solvents; even though clay particles were also observed, its size was lower (90–529 nm). It is expected that as far as particle size becomes lower, mechanical properties are better, but it must be noted that SEM resolution does not allow seeing intercalated or exfoliated clay layers. Analyzing the different clay contents in the optimal conditions, significant differences in SEM micrographs were not observed and the range of particles size was 90–390 nm.

3.2. PCL/clay nanocomposite films obtained by intensive mixing

3.2.1. Mechanical properties

Table 5 shows mechanical properties for the matrix and for the 2.5C30B, 5C30B and 7.5C30B nanocomposites prepared by intensive mixing. The highest Young's modulus was achieved with 5C30B nanocomposites. It resulted 70% higher with respect to the matrix, although strength and elongation at break were 21% and 24% lower, respectively.

In contrast to casting results, all nanocomposites exhibited improved Young's modulus in comparison to the matrix since

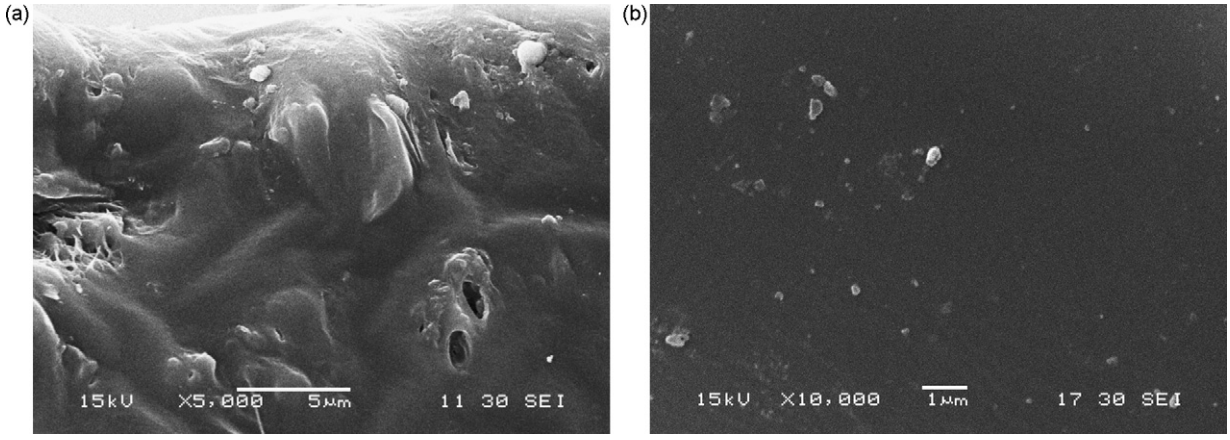

Fig. 5. SEM micrographs of 5C30B nanocomposite films thickness at 15 min ultrasonic bath: (a) dichloromethane and (b) mixing of solvents.

Table 5
Mechanical properties and degree of crystallinity from DSC analysis for matrix and their clay nanocomposites prepared by intensive mixing

Material	Young's modulus (MPa)	Strength (MPa)	Elongation at break (%)	ΔH_f (J/g)	X_{cr} (%)
PCL	452 ± 66	53.5 ± 0.5	872 ± 144	81.11	57
2.5C30B	574 ± 5	37 ± 6.0	580 ± 81	89.20	64
5C30B	767 ± 61	42 ± 9.0	657 ± 42	74.34	55
7.5C30B	757 ± 56	39.3 ± 2.5	760 ± 70	71.59	55

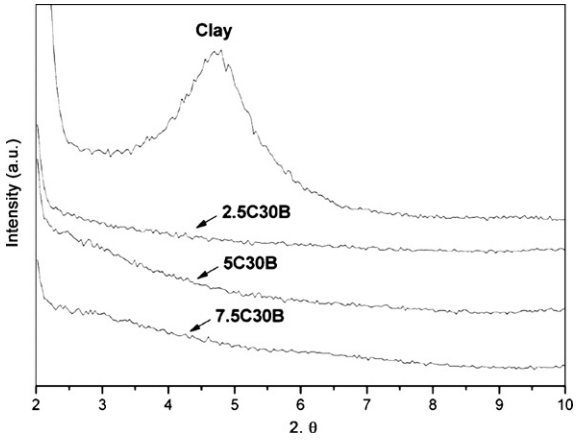

Fig. 6. X-ray diffractograms for nanocomposites prepared by intensive mixing.

no defects were observed in the evaporation surface either by optical or SEM microscopy.

3.2.2. Crystallinity

Table 5 shows the degree of crystallinity for PCL and their clay nanocomposites prepared by intensive mixing. The degree of crystallinity remained almost unchanged in the presence of clay.

3.2.3. Nanocomposite structure

Fig. 6 shows X-ray diffractograms for the nanocomposites prepared by intensive mixing. A mixture of both clay structures, intercalated and exfoliated, was achieved with all clay contents studied. In this case, analyzing the films thickness by SEM, defects and clay particles were not observed in the nanocomposites.

3.3. Comparison between nanocomposites prepared by casting and intensive mixing

Table 6 shows the mechanical properties in comparison to the neat matrix for the best nanocomposites obtained by each technique. The improvement of these properties is related to clay platelets dispersion in the polymer, which depends on both components interaction and the processing technique [15]. It has been stated that intensive mixing is an excellent technique to obtain nanocomposites with high mechanical properties in comparison to the neat polymer [16]. When clay is blended with the polymer melt, the shear forces induced in the mixer produce clay platelets separation, and a high degree of dispersion could be achieved depending on the interactions between components [17].

It was shown that clay particles have a detrimental effect on strength that can be attributed to a bad clay/polymer interaction. If this is the case, a good dispersion of the particles may be reached as a result of strong shear forces during mixing but the system, however, remains unstable [6]. Table 6 reveals that shear forces induced in the mixer in intensive mixing method, in comparison to the ultrasonic bath and the solvent used in casting, are more important for the mechanical properties improvements of PCL/C30B nanocomposites. Therefore, it is evident that the shear stress makes a positive contribution to the mechanical properties. It must be noted that if such an unstable mixture is heated to temperatures above the polymer melting point, a (partial) re-agglomeration of the particles can take place [6]. This could be the case of obtaining films by compression molding after mixing. By comparing both techniques in the nanocomposites mechanical properties improvements or detriments with respect to the neat matrix (Table 6), it can be concluded that the defects introduced during solvents evaporation in casting produce worse effects on mechanical properties than partial re-agglomeration during compression molding.

Clay particles had a detrimental effect not only on strength but also on ductility as they may be immobilizing the polymer chains decreasing the polymer ductility.

3.4. Modelling mechanical properties

3.4.1. Halpin–Tsai micromechanics-based model

Micromechanics-based composite models have been used to examine how filler structural parameters (e.g. shape, aspect ratio and orientation) affect the mechanical properties of a neat matrix [18,19]. Although these micro-mechanical models cannot be used to fully account for the exact mechanical behav-

Table 6
Comparison between best mechanical properties achieved by each technique of nanocomposites preparation

Technique	Young's modulus, $[(E - E_m)/E_m] \times 100$ (%)	Strength, $[(\sigma - \sigma_m)/\sigma_m] \times 100$ (%)	Elongation at break, $[(\varepsilon - \varepsilon_m)/\varepsilon_m] \times 100$ (%)
Casting	+47	−40	−33
Intensive mixing	+70	−21	−24

m is related to the matrix.

Table 7
Constant parameters used in the effective filler-based micromechanical model

Technique	E_m (MPa)	E_f (GPa) [22]	t_p (nm) [22]	l (nm) [22]	ρ_m (g/cm^3) [22]	ρ_f (g/cm^3) [22]
Casting	405	180	1	110	1.2	1.98
Intensive mixing	452	180	1	110	1.2	1.98

ior of polymer nanocomposites, it generally gives satisfactory correlations.

In conventional micromechanical models, filler volume fraction (ϕ_f), aspect ratio (α), orientation (S), and modulus (E_f) are important factors for describing the macroscopic composite properties. Tucker and Liang [20] reviewed the application of several models for fiber-reinforced composites. They reported that the Halpin–Tsai theory [21] offered reasonable predictions for composite modulus. The longitudinal engineering modulus (E_{11}) of the Halpin–Tsai model is expressed in the following equation:

$$\frac{E_{11}}{E_m} = \frac{1 + 2(l/t_p)\eta\phi_f}{1 - \eta\phi_f} \tag{3}$$

where l is the filler length, E_m the Young's modulus of the matrix and t_p is the filler thickness and:

$$\eta = \frac{(E_f/E_m) - 1}{(E_f/E_m) + 2(l/t_p)} \tag{4}$$

3.4.2. *Effective filler-based micromechanical models proposed by Weon and Sue [22]*

The dispersion of clay in a matrix can be described as exfoliation or intercalation. Conventional filler-based micromechanical models for predicting the modulus of nanocomposites do not consider the clay structural characteristics. Weon and Sue [22] defined typical clay structural parameters by the number of platelets per stacked clay (n) and the interlayer spacing (d_{001}). These parameters can be used to predict the Young's modulus either for exfoliated or intercalated systems. In this case, conventional parameters (α, ϕ_f and E_f) must be expressed in terms of the effective structural parameters (n, d_{001}).

The thickness of the effective filler (t_{eff}) can be expressed by the following equation [19]:

$$t_{eff} = (n - 1)d_{001} + t_p \tag{5}$$

The effective filler aspect ratio (α_{eff}), the volume fraction (ϕ_{eff}) and the modulus (E_{eff}) can be written as [18]:

$$\alpha_{eff} = \frac{l}{t_{eff}} = \frac{l}{(n - 1)d_{001} + t_p} \tag{6}$$

$$\phi_{eff} = \frac{\psi_{eff}[(n - 1)d_{001} + t_p]}{nt_p}\frac{\rho_m}{\rho_f} \tag{7}$$

$$E_f^{eff} = \frac{nt_pE_f}{[(n - 1)d_{001} + t_p]} \tag{8}$$

where ψ_{eff} is the effective filler weight fraction and ρ_f, ρ_m are filler and matrix densities, respectively.

In this work the effective filler-based micromechanical model proposed by Weon et al. was used to predict the degree of dispersion of nanocomposites based on the experimental Young's modulus values. The platelets length (l) value reported by Weon and Sue [22] was used. The number of platelets per stacked clay (n) would not be exact using this approximation, so a relative n value was used in order to make a comparison of the dispersion degree between the different nanocomposites. The relative value (n_r) was determined by the following equation:

$$n_r = \frac{n_i}{n_{min}} \tag{9}$$

where n_i is the n value for different weight percents of clay and n_{min} is the lowest n value. It must be noted that n_i and n_{min} are related to the same preparation technique.

Before replacing t_{eff}, α_{eff}, ϕ_{eff} and E_{eff} in Eqs. (3) and (4) and expressing E_{11}/E_m as a function of ψ_{eff}, the number of platelets per stacked clay (n) becomes the only unknown parameter. The constant parameters used can be seen in Table 7.

Table 8
Relative number of platelets per stacked clay (n_r) from the effective filler-based micromechanical model

Material	n_r	
	Casting	Intensive mixing
2.5C30B	–	1.3
5C30B	1.6	1.0
7.5C30B	10.0	1.7
10C30B	47.0	–

Table 8 shows n_r values, which resulted from mechanical properties modelling. In the case of casting method, particles agglomeration begins at 7.5 wt.% of clay. It can be noted that the dispersion degree for intensive mixing was higher than for casting. Therefore, we conclude that intensive mixing is a more effective technique to prepare PCL/C30B nanocomposites because it did not introduce defects in the surface and the dispersion degree resulted higher. These conclusions are both critical to obtain good mechanical performance.

4. Conclusions

Analyzing the nanocomposites prepared by both techniques we can point out several remarkable ideas that are following detailed.

A mixed clay structure, intercalated and exfoliated, coexisted in nanocomposites prepared by techniques, intensive mixing and casting.

The solvent choice and evaporation procedure for casting method is of crucial importance since it could produce holes during its evaporation, which is the case of dichloromethane in the present study. Other important factors are the ultrasonic bath

time and the clay content being 15 min and 5 wt.% the optimal conditions for the PCL/C30B nanocomposites.

With the first used conditions (150 rpm, 10 min, 100 °C) in intensive mixing, the mechanical properties were superior to those of the films obtained by casting. This can be associated to the shear forces developed in the intensive mixer. For this technique the highest modulus was obtained for 5 wt.% of C30B.

The relative dispersion degree estimated from the effective-filler parameter model was higher for intensive mixing. This result together with the morphological study and the mechanical properties seemed to show that the shear forces built up during processing are better than the solvent effect to obtain well-dispersed PCL/C30B nancomposites and to achieve, consequently, a good mechanical performance.

In addition, the absence of solvent, which can produce environmental problems is another advantage for the intensive mixing technique.

Acknowledgements

The authors acknowledge CONICET (PIP 6254), Antorchas Foundation and ANPCyT-Proyecto FONCyT-PICT 03-no. 12-15074 for the financial support.

References

[1] B. Lepoittevin, M. Devalckenaere, N. Pantoustier, M. Alexandre, D. Kubies, C. Calberg, R. Jérôme, P. Dubois, Polymer 43 (2002) 4017–4023.
[2] P. Christian, I.A. Jones, Polymer 42 (2001) 3989–3994.
[3] P. Dubois, C. Jacobs, R. Jerome, P. Teyssie, Macromolecules 24 (1991) 2266–2270.
[4] P.B. Messersmith, E.P. Giannelis, Chem. Mater. 5 (1993) 1064–1066.
[5] M. Alexandre, P. Dubois, Mater. Sci. Eng. R: Rep. 28 (2000) 1–63.
[6] F. Hartmut, Mater. Sci. Eng. C 23 (2003) 763–772.
[7] G. Lagaly, Appl. Clay Sci. 15 (1999) 1–9.
[8] W. Jinghe, M. Michael, Chem. Mater. 5 (1993) 835–838.
[9] G. Jimenez, N. Ogata, H. Kawai, T. Ogihara, J. Appl. Polym. Sci. 64 (1997) 2211–2220.
[10] G. Gorrasi, M. Tortora, V. Vittoria, E. Pollet, B. Lepoittevin, M. Alexandre, P. Dubois, Polymer 44 (2003) 2271–2279.
[11] D. Homminga, B. Goderis, S. Hoffman, H. Reynaers, G. Groeninckx, Polymer 46 (2005) 9941–9954.
[12] W.Y. Yam, J. Ismail, H.W. Kammer, H. Schmidt, C. Kummerlöwe, Polymer 40 (1999) 5545–5552.
[13] D. Burgentzlé, J. Duchet, J.F. Gérard, A. Jupin, B. Fillon, J. Colloid Interf. Sci. 278 (2004) 26–39.
[14] A.G. Simanke, G.B. Galland, L. Freitas, J.A.H. da Jornada, R. Quijada, R.S. Mauler, Polymer 40 (1999) 5489–5495.
[15] E. Chabert, M. Bornert, E. Bourgeat-Lami, J.Y. Cavaillé, R. Dendievel, C. Gauthier, J.L. Putaux, A. Zaoui, Mater. Sci. Eng. A 381 (2004) 320–330.
[16] J. Xu, R.K.Y. Li, Y.Z. Meng, Y.W. Mai, Mater. Res. Bull. 41 (2006) 244–252.
[17] J. Jordan, K.I. Jacob, R. Tannenbaum, M.A. Sharaf, I. Jasiuk, Mater. Sci. Eng. A 393 (2005) 1–11.
[18] N. Sheng, M.C. Boyce, D.M. Parks, G.C. Rutledge, J.I. Abes, R.E. Cohen, Polymer 45 (2004) 487–506.
[19] T.D. Fornes, D.R. Paul, Polymer 44 (2003) 4993–5013.
[20] C.L. Tucker, E. Liang, Compos. Sci. Technol. 59 (1999) 655–671.
[21] J.C. Halpin, J.L. Kardos, Polym. Eng. Sci. 16 (1976) 344–352.
[22] J.I. Weon, H.J. Sue, Polymer 46 (2005) 6325–6334.